Modeling and Simulation of Micro-Manipulator Robotic System for Neurosurgery

Ya'akob Yusof and **M. R. Arshad**

Underwater Robotics Research Group (URRG), School of Electrical and Electronics Engineering,
Universiti Sains Malaysia, Engineering Campus,
14300 Nibong Tebal, Seberang Perai Selatan, Pulau Pinang, Malaysia
Tel: +604-5937788
E-mail: aqoubm@gmail.com, rizal@eng.usm.my

Abstract

This research focuses on modeling and control simulation of a micro-manipulator robotic system model for neurosurgery application. A highly reliable controller is vital in this type of system. In order to design the controller, we need to initially know the behavior of the whole system, which is its kinematics and dynamic characteristics. This paper first presents the model of this robot using Robotics Toolbox™. Then, it simulates the kinematics model of the micro-manipulator, as well as the dynamic analysis of it. The workspace of the robot is also drawn in order to understand the capability of the micro-manipulator. Lastly, we apply two control techniques on the micro-manipulator model, which are computed torque control and PID-computed torque control and make a comparison of the results. From the controller implementation results, PID-computed torque control controller emerged as a much better control technique for the micro-manipulator model due to the additional terms to the input of the controller design which reduce the tracking errors. In addition, PID-computed torque control method reaches its steady-state faster than computed torque control. For future works, employing a more robust controller that has the capability to smoothen sharp corners and reduce disturbances is considered vital for the success of this manipulation system.

Keywords:

Neurosurgery, micro-manipulator, Robotics Toolbox™, manipulator kinematics, dynamic model, computed torque control, PID-computed torque control.

1. Introduction

Neurosurgery is a part of the surgical field that focused in taking care of the diseases related to human's central peripheral nervous system and also their central spinal cord [1]. The term surgery refers to the operation of peripheral nervous system as well as the spinal cord; brain, blood vessel connected to it, spine, spinal cord, and also nerves that control our senses and body's movement [2]. There are lots of neuro diseases, which among them termed as brain tumors, head trauma, stroke, and spinal cord trauma.

Why did robot need to be involved in neurosurgery? According to [3], the advantages of using robots are in terms of its efficiency in costs incurred, to minimize the effect of doctor's fatigue and for the patient to experience less trauma for the incision being made to through their body. According to [4], the first involvement of robot in a neuro related surgery was reported in 1985. Although the robot at that operation only holds the biopsy cannulae, it started the great length of robots involvement in neurosurgery. The involvement of robots in surgical application has made its great impressive runs. The researches going on in this topic is wide as well. Jingke et al [5] in their research designed an assisting robotic arm to help the surgeon in a minimally invasive surgery (MIS) for breast operation. This robotic arm used a mechanism called ball-joint-brake. The mechanism has high dexterity and small physical volume requirement of the wrist joint. In addition, Kanako et al [6] introduced a new surgical tool for intrauterine fetal surgery in an open MRI (magnetic resonance imaging). Invented to deal with the common fetal diseases such as myelomeningocele, this robotic tool is one of the smallest ever developed micro-manipulator with 2.4mm in its diameter, and can be bend to as tiny as 2.45mm radius. This smallness is really a great feature that my research is going to look into, because the smaller the tools will result in smaller incision in patients head, thus minimizing the trauma they need to face.

In dealing with surgical procedure, including neuro related surgery, precision and accuracy plays a very important role. This leads to the needs of micro-manipulation. Micro-manipulation refers to object handling in micro scale [7]. This explains that the level of manipulation is very small and the accuracy in need is very high. Not just the tool and manipulator must be small or micro, the controller for this system must be good to be able to produce a very precise motion with a very minimal error in all the 3-axis's direction. Controller design process is actually the most important aspect in this research, as it will act as the brain for the whole system.

In this paper, we will briefly explain the model of the micro-manipulator that has been used for our modeling and analysis process. The kinematics and dynamic analysis will be performed on this micro-manipulator model. Moreover, we will implement two control techniques on the model and simulate the performances. From the two controllers, we want to find which control technique can provide us with the least and smallest tracking error possible for the selected model of micro-manipulator. Results from this controller implementation will be discussed.

2. Approach and Method

2.1 Robotics Toolbox™ (RT)

RT is one of the various MATLAB Toolboxes that allow its users to understand and implements theoretical concepts in robotics through insightful simulation and visualization [8]. It is able to model and simulate a robot's kinematics and dynamics, as well as the orientation and trajectory generation of the model defined [9]. Moreover, with it available in form of Simulink's block diagrams, it can be used with other powerful toolboxes such as Control System Toolbox and Machine Vision Toolbox, which is making it a very useful tool for further operations such as various analysis and controller design processes. RT represents the robot using Denavit Hartenberg parameters. The parameters have two general conventions, standard and modified (termed as DH and MDH, respectively) version. Both can be model in RT, but we have to be careful when using the link transformation's matrix and other properties in the modeling and analysis process, as there are some differences in declaration of both conventions.

In this paper, RT and Simulink will be used in modeling the micro-manipulator, as well as for all analysis and controller implementation process. The connection features available with other useful toolboxes in MATLAB made the whole project much at ease.

2.2 Micro-Manipulator Modeling

The micro-manipulator that is going to be modeled, as well as its considered parameters, is a 6-DOF manipulator that has been obtained from F. Cepolina in [10]. It has one redundant DOF for the end effector. However, in the modeling process, this redundant DOF is assumed to be outmoded with the last joint of the manipulator. Figure 1 shows the micro-manipulator, in a CAD drawing, that is going to be modeled and analyzed.

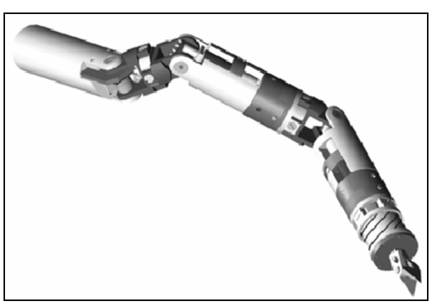

Figure 1: The micro-manipulator

This micro-manipulator model has been chosen because of its size which is very small. This can ease few tasks, for example it can be put very close to a patient's body and reduce tools' vibration during procedure. Moreover, its workspace area, which is later shown in Figure 4, is small and suitable for a neurosurgery operation. This made it able to go with a fine and precise motion during operation, of course with the help of a good controller working with it.

In modeling process, DH is a common method to represents the robotic model in terms of size and orientation of the robotic links. In the modeling of the micro-manipulator in this work, we analyzed it using the modified version of DH, termed as MDH. We choose MDH as it is easier for us in terms of understanding to model it using MDH, as compared to DH. RT can accommodate both DH and MDH.

2.3 Links' Transformation Matrices

When we have the MDH parameters, link transformation's matrix can be formed, according to [11]. This links transformation matrices were important for further kinematics and analysis of the manipulator. In general, link's transformation matrix is given by equation (1).

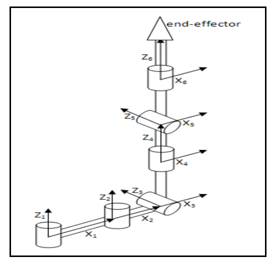

Figure 2: Geometric model of the micro-manipulator, with all the frame assignments

$$ {}^{i-1}T_i = \begin{bmatrix} \cos\theta_i & -\sin\theta_i & 0 & a_{i-1} \\ \sin\theta_i \times \cos\alpha_{i-1} & \cos\theta_i \times \cos\alpha_{i-1} & -\sin\alpha_{i-1} & -\sin\alpha_{i-1} \times d_i \\ \sin\theta_i \times \sin\alpha_{i-1} & \cos\theta_i \times \sin\alpha_{i-1} & \cos\alpha_{i-1} & \cos\alpha_{i-1} \times d_i \\ 0 & 0 & 0 & 1 \end{bmatrix} \quad (1) $$

2.4 Workspace Area

To calculate and draw the workspace of the end-effector of the micro-manipulator, we need to have the kinematic equations representing the motion of the end-effector. Since we have six joints, equation (2) defines the kinematic equations for this micro-manipulator model.

$$ {}^0T_6 = {}^0T_1 \times {}^1T_2 \times {}^2T_3 \times {}^3T_4 \times {}^4T_5 \times {}^5T_6 \quad (2) $$

2.5 Trajectory Planning

Trajectory described the motion of the micro-manipulator in 3-D space. It represents time history of position, velocity and acceleration for each joint, whether it is revolute or prismatic. Equation 3 represents the trajectory equation for every joint [12]. The trajectory is in angular displacement. Here, five-order polynomials are used because we want to implement path segments. From path segments, we will be able to specify the position, velocity and acceleration at any time or segments. This is important for the system because we need to specify each and every point on the route of the end-effector. Failing to do this might affect unnecessary nerves or tissue. Other n-degree polynomials can be used, but it depends on the number of constraints we are having and the results we wanted. For example, if we use three-order polynomials, we cannot have smoother functions that represent the position, velocity and acceleration of the system.

$$\theta(t) = c_0 + c_1 t + c_2 t^2 + c_3 t^3 + c_4 t^4 + c_5 t^5 \quad (3)$$

Therefore, the velocity and acceleration (angular);

$$\dot{\theta}(t) = c_1 + 2c_2 t + 3c_3 t^2 + 4c_4 t^3 + 5c_5 t^4 \quad (4)$$

$$\ddot{\theta}(t) = 2c_2 + 6c_3 t + 12c_4 t^2 + 20c_5 t^3 \quad (5)$$

Equation (6) below represents the all the coefficients of the polynomials, c_i;

$$\begin{aligned} c_0 &= \theta_0 \\ c_1 &= \dot{\theta}_0 \\ c_2 &= \frac{\ddot{\theta}_0}{2} \\ c_3 &= \frac{20\theta_f - 20\theta_0 - (8\dot{\theta}_f + 12\dot{\theta}_0)t_f - (3\ddot{\theta}_0 - \ddot{\theta}_f)t^2{}_f}{2t^3{}_f} \\ c_4 &= \frac{30\theta_0 - 30\theta_f + (14\dot{\theta}_f + 16\dot{\theta}_0)t_f + (3\ddot{\theta}_0 - 2\ddot{\theta}_f)t^2{}_f}{2t^4{}_f} \\ c_5 &= \frac{12\theta_f - 12\theta_0 - (6\dot{\theta}_f + 6\dot{\theta}_0)t_f - (\ddot{\theta}_0 - \ddot{\theta}_f)t^2{}_f}{2t^5{}_f} \end{aligned} \quad (6)$$

2.6 Dynamic Model

During operation, manipulator will experience acceleration and increasing in velocity, deceleration and decreasing in velocity, as well as constant speed where the acceleration is zero. This time-varying activities are termed as its dynamic behavior. As a result, time-varying torques are applied at the joints, in reaction to the internal and external forces which caused by motion of links and forces exerted by environment, respectively. This resultant torques vector will definitely be transferred to a human's head during operation, thus proper control of the produced torques are also important.

The way how the micro-manipulator behaves in response to those internal and external torques are known as equations of motion, as stated in equation (7), given by [13]&[14];

$$\tau = M(\theta)\ddot{\theta} + C(\theta,\dot{\theta})\dot{\theta} + N(\theta,\dot{\theta}) \quad (7)$$

where;

τ = torques vector

M = inertia matrix

C = Coriolis and Centrifugal matrix (these are types of internal forces)

N = gravity terms and other forces act on the joints (all external forces defines here)

2.7 Computed Torque Control (CTC)

CTC is a control method that applies feedback linearization to nonlinear systems [15]. This control technique is chosen because it provides the system with better trajectory-tracking performance than of a normal linear controller. The general mathematical expression of this controller is given below.

Given that the feedback for CTC technique;

$$\ddot{\theta} = \ddot{\theta}_d + K_D(\dot{\theta}_d - \dot{\theta}) + K_P(\theta_d - \theta) \quad (8)$$

Substituting equation (8) into equation (7), the overall controlled input torque is given by;

$$\tau = M(\theta)[\ddot{\theta}_d + K_D(\dot{\theta}_d - \dot{\theta}) + K_P(\theta_d - \theta)] + \ldots \\ \ldots C(\theta,\dot{\theta})\dot{\theta} + N(\theta,\dot{\theta}) \quad (9)$$

where;

$\ddot{\theta}_d$ = current value of $\ddot{\theta}$ during iteration

$\dot{\theta}_d$ = current value of $\dot{\theta}$ during iteration

θ_d = current value of θ during iteration

K_D, K_P = derivative and proportional gain

2.7 PID - Computed Torque Control (PID-CTC)

Here, we add an integral term from the above control technique, as defined in [16]. The feedback becomes;

$$\ddot{\theta} = \ddot{\theta}_d + K_D(\dot{\theta}_d - \dot{\theta}) + K_P(\theta_d - \theta) + \ldots \\ \ldots K_I \int (\theta_d - \theta)dt \quad (10)$$

Substituting equation (10) into equation (7), the overall controlled input torque is given by;

$$\tau = M(\theta)[\ddot{\theta}_d + K_D(\dot{\theta}_d - \dot{\theta}) + K_P(\theta_d - \theta) + \ldots \\ \ldots K_I \int (\theta_d - \theta)dt] + C(\theta,\dot{\theta})\dot{\theta} + N(\theta,\dot{\theta}) \quad (11)$$

where K_I =integral gain.

3. Results and Discussion

3.1 Micro-Manipulator Model

The MDH parameters were represented in Table 1. These parameters were derived based on the geometric model and frame assignment of the manipulator in Figure 2. In the frame assignment, the y-axis was not shown for illustration purpose. The lengths of the manipulator's links are given as L1=50mm, L2=15mm, L3=36mm, and L4=39.5mm. These lengths were taken from the original model. From all the information, the micro-manipulator is modeled using RT. The resulting model drawn by RT is shown in Figure 3.

Joint # (i)	**α_{i-1} (degree)**	**a_{i-1} (mm)**	**Θ_i (degree)**	**d_i (mm)**	**Links' notation ($^{i-1}T_i$)**
1	0	0	Θ_1	0	$^0T_1$
2	0	L_1	Θ_2	0	$^1T_2$
3	-90	L_2	Θ_3	0	$^2T_3$
4	90	0	Θ_4	L_3	$^3T_4$
5	-90	0	Θ_5	0	$^4T_5$
6	90	0	Θ_6	L_4	$^5T_6$

Table 1: Parameters for Modified DH (MDH) table

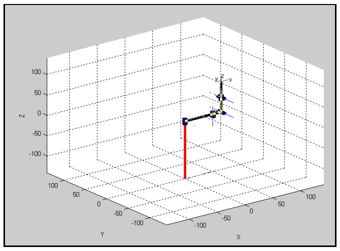

Figure 3: RT's model of the micro-manipulator.

3.2 Links' Transformation Equation

From equation (1), after substituting all the parameters from the MDH table, we have six matrices, to represents all the six links we have for the micro-manipulator.

$$^{0}\mathrm{T}_1 = \begin{bmatrix} \cos\theta_1 & -\sin\theta_1 & 0 & 0 \\ \sin\theta_1 & \cos\theta_1 & 0 & 0 \\ 0 & 0 & 1 & 0 \\ 0 & 0 & 0 & 1 \end{bmatrix} \quad (12)$$

$$^{1}\mathrm{T}_2 = \begin{bmatrix} \cos\theta_2 & -\sin\theta_2 & 0 & 50 \\ \sin\theta_2 & \cos\theta_2 & 0 & 0 \\ 0 & 0 & 1 & 0 \\ 0 & 0 & 0 & 1 \end{bmatrix} \quad (13)$$

$$^{2}\mathrm{T}_3 = \begin{bmatrix} \cos\theta_3 & -\sin\theta_3 & 0 & 15 \\ 0 & 0 & 1 & 0 \\ -\sin\theta_3 & -\cos\theta_3 & 0 & 0 \\ 0 & 0 & 0 & 1 \end{bmatrix} \quad (14)$$

$$^{3}\mathrm{T}_4 = \begin{bmatrix} \cos\theta_4 & -\sin\theta_4 & 0 & 0 \\ 0 & 0 & -1 & -36 \\ \sin\theta_4 & \cos\theta_4 & 0 & 0 \\ 0 & 0 & 0 & 1 \end{bmatrix} \quad (15)$$

$$^{4}\mathrm{T}_5 = \begin{bmatrix} \cos\theta_5 & -\sin\theta_5 & 0 & 0 \\ 0 & 0 & 1 & 0 \\ -\sin\theta_5 & -\cos\theta_5 & 0 & 0 \\ 0 & 0 & 0 & 1 \end{bmatrix} \quad (16)$$

$$^{5}\mathrm{T}_6 = \begin{bmatrix} \cos\theta_6 & -\sin\theta_6 & 0 & 0 \\ 0 & 0 & -1 & -39.5 \\ \sin\theta_6 & \cos\theta_6 & 0 & 0 \\ 0 & 0 & 0 & 1 \end{bmatrix} \quad (17)$$

3.3 Workspace Area

Joint	Θ_{left} (degree)	Θ_{right} (degree)
1	-180	180
2	-90	90
3	0	180
4	-180	180
5	-90	90
6	-180	180

Table 2: Joints' limit for rotation of each links of the micro-manipulator for workspace area

From equation (2), we can have the kinematic equations representing the position of the end-effector, as well as the orientation of it. However, in plotting the workspace of the manipulator, we will only consider the position of the end-effector, which is the last column of the matrices. Other columns represent the orientation of the end-effector. In addition, we need to as well consider the joints' limit as shown in Table 2. Equation (18) shows the kinematic equations of the end effector (for workspace calculation);

$$\begin{bmatrix} P_x \\ P_y \\ P_z \\ Z \end{bmatrix} = \begin{bmatrix} 39.5(((c_1c_2 - s_1s_2)c_3c_4 + (-c_1s_2 - s_1c_2)s_4)s_5 + (c_1c_2 - s_1s_2)s_3c_5 + \ldots \\ 39.5(((s_1c_2 + c_1s_2)c_3c_4 + c_1c_2 - s_1s_2)s_4)s_5 + (s_1c_2 + c_1s_2)s_3c_5) + \ldots \\ 39.5(c_3c_5 - s_3c_4s_5) + 36(c_3) + \ldots \\ 1 + \ldots \end{bmatrix}$$

$$\begin{bmatrix} \ldots 36(c_1c_2 - s_1s_2)s_3 + 15(c_1c_2 - s_1s_2) + 50(c_1) \\ \ldots 36(s_1c_2 + c_1s_2)s_3 + 15(s_1c_2 + c_1s_2) + 50(s_1) \\ \ldots 0 \\ \ldots 0 \end{bmatrix}$$

… (18)

where;

$c_i = \cos\theta_i$, and $s_i = \sin\theta_i$.

Using graphical plotting software, we plot the workspace of the micro-manipulator. Figure 4 represents the workspace of the end –effector, which has a form of dotted clouds.

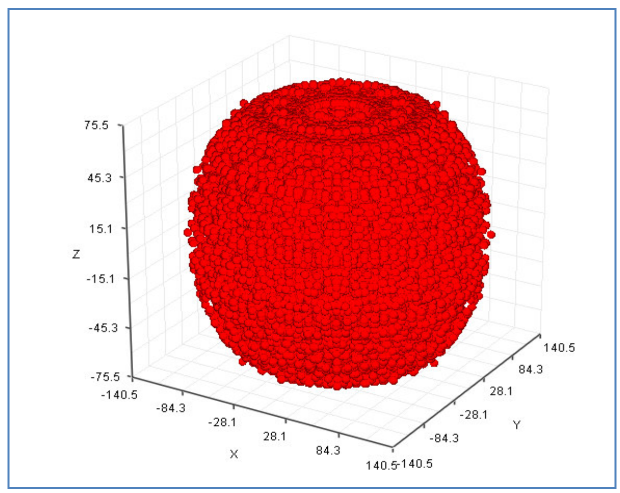

Figure 4: Workspace of the end-effector. The dimension is in mm in all axes

3.4 Trajectory Generation

To plot the trajectory, we must define the starting and end points of the joints over certain range of time and see the results. Using MATLAB, the trajectory of the joints was calculated and plotted as in Figure 5, taking joints 1 and 5 as example.

3.5 Dynamic Model

Torques at each joints were also plotted over the same trajectories and time range. The torques plotted was shown in Figure 6. Torques applied at the joints was also to balance out the internal and external forces acting on them.

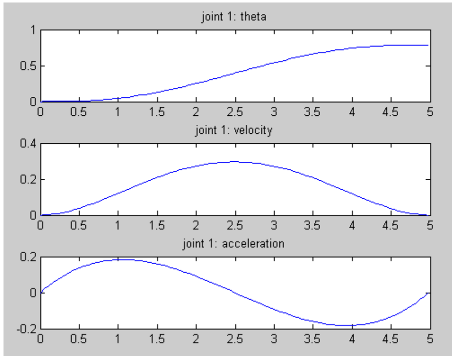

5(a)

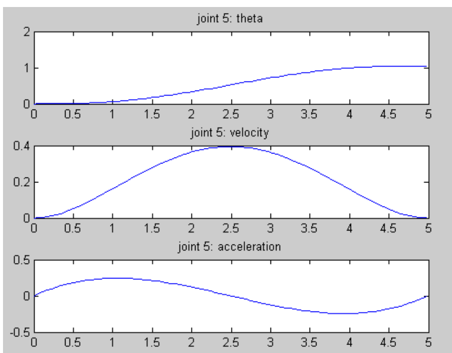

5(b)

Figure 5: Trajectories for joints 1 and 5 is shown in Figure 5(a) and Figure 5(b), respectively. The units for position (theta) = radians (rad), velocity = rad·s^{-1} and acceleration = rad·s^{-2}

3.6 Controller Implementation and Analysis

To further analyze and simulate the performance of the micro-manipulator that has been modeled, we implement few controller onto it and monitor its performance. Two types of controller method have been chosen, the CTC and PID-CTC. Basically, both control strategy employ computed torque's algorithm, but in the second control strategy, we add an integral part into it to observe its performance.

Using Simulink, the desired trajectories of each of the six joints were plotted as shown in Figure 7. The trajectories as in Figure 5 were sent to the micro-manipulator model and see how well the manipulator follows the given trail. The outcome is shown in Figure 8. It shows that when the actuators acting about the micro-manipulator, its performance cannot be easily defined without any supervision or control. From here, it is clearly acknowledged that we need a controller for the system, in order to make sure the micro-manipulator did the right job and follow the right path. The results in Figure 8 were also due to the internal and external forces acting on the manipulator, as a result of the movement of each link with respect to each other, which deviates the system.

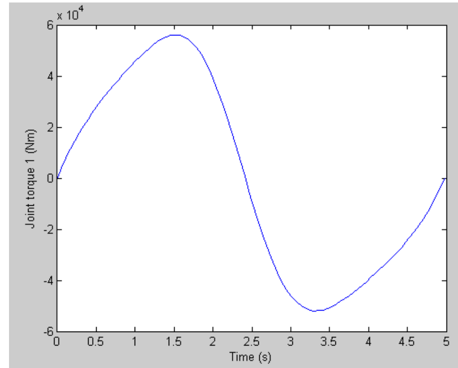

6(a)

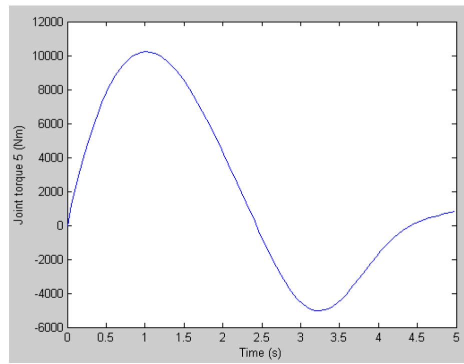

6(b)

Figure 6: Torques applied at joints 1 and 5 is shown in Figure 6(a) and Figure 6(b), respectively

Using Simulink blocks and RT, the resulting trajectories of the micro-manipulator with CTC technique applied on it is shown in Figure 9. The result shows that the trajectories are better than Figure 8. However, there is still room for improvement.

Using the same method, the results when PID-CTC controller was implemented on the micro-manipulator model are shown in Figure 10.

Figures 11 and 12 shows the tracking error obtained from the first and fifth joints following the desired trajectory of both CTC and PID-CTC control. From the results, it is clearly shows that PID-CTC is a better controller for this micromanipulator model than CTC control technique. The tracking errors' values for PID-CTC are very small compared to CTC for both joints. This is due to the differences of algorithm used. PID-CTC adds additional terms to the input which reduce the tracking errors. The additional term, K_I is crucial to the controller design in order to get better results. In addition to that, from Figure 11 and 12, the PID-CTC method reaches its steady-state faster than CTC.

Even though PID-CTC gave better results, its simulation processing time takes longer than CTC. PID-CTC took 125 seconds and about 380 iterations to complete the whole process, while CTC took 76 seconds and about 200 iterations.

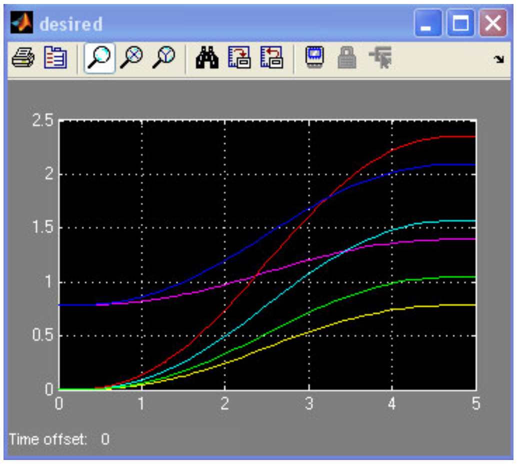

Figure 7: Desired trajectories of each joint (angle, in radian)

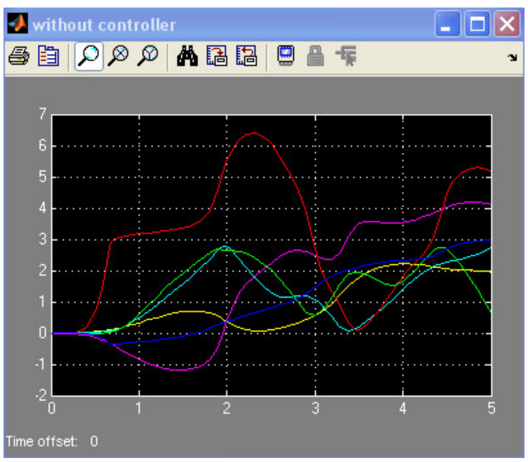

Figure 8: Robot's joint trajectory (angle, in radian) without any controller applied

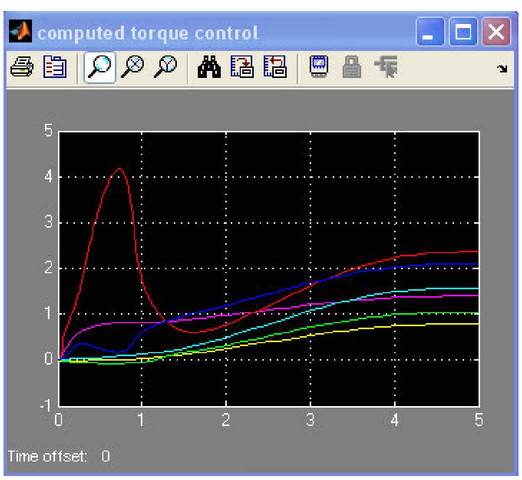

Figure 9: Micro-manipulator's joints' trajectory (angle, in radian) with CTC is shown on the right

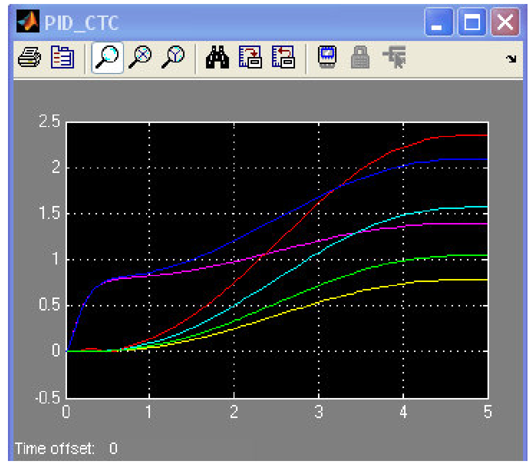

Figure 10: Micro-manipulator's joints' trajectory (angle, in radian) with PID-CTC is shown on the right

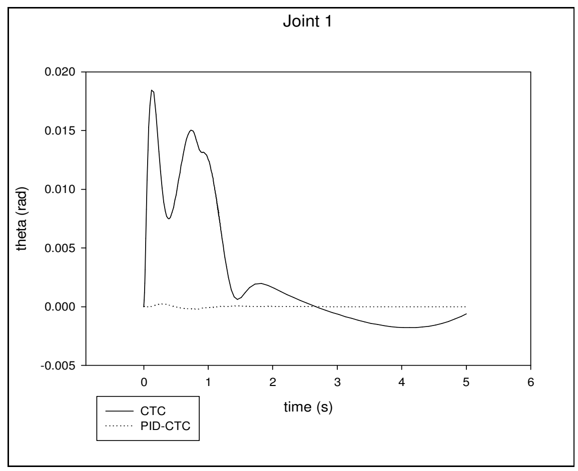

Figure 11: Tracking error for both CTC and PID-CTC at joint 1

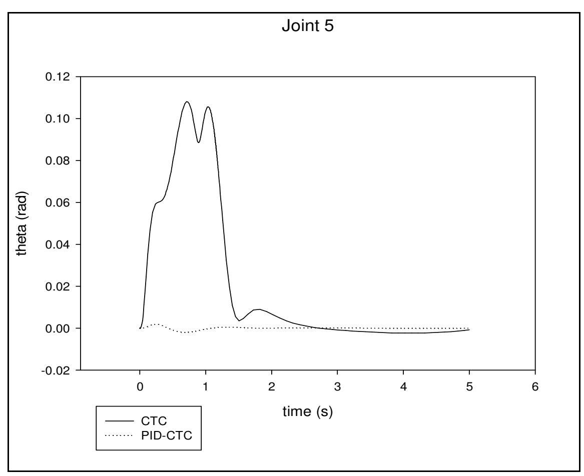

Figure 12: Tracking error for both CTC and PID-CTC at joint 5

4. Conclusion

This paper described the modeling and simulation of a robotic micro-manipulator's model and controller implementation for neurosurgery purposes. From the kinematics and dynamic analysis, we have been able to understand the behavior of the micro-manipulator model. Furthermore, from the controller implementation results, PID-CTC controller emerged as a much better control technique for the micro-manipulator model as it provides us with very small tracking error, as compared to CTC technique. This is due to the additional terms to the input of the controller design, K_I which reduce the tracking errors. This is crucial to the controller design in producing better results. Furthermore, it is clearly seen that PID-CTC method reaches its steady-state faster than CTC, even though it takes longer time to complete the iterations.

4.1 Future Works

The tasks defined above are considered not enough as it does not involved sharp or severe corners or path, and no disturbances applied. However, in real application, those criteria need to be considered. Thus, employing a more intelligent controller that has the capability to smoothen sharp corners and reduced any disturbances during the operation is considered vital for the success of the manipulation system. With the aim that this micro-manipulator will operate on a person's head, an excellent or robust controller is much more in need.

5. Acknowledgments

This 'Robotic Micro-Manipulator for Neurosurgery' project is funded by Escience Fund from the Ministry of Science, Technology and Innovation (MOSTI).

References

[1] Wikipedia; *Neurosurgery*, http://en.wikipedia.org/wiki/Neurosurgery

[2] Sanjay Mongia (Dr.); *What is Neurosurgery*, http://www.neurosurgeon.co.in/neurosurgery.html

[3] *How Robotic Surgery will Work*, http://science.howstuffworks.com/robotic-surgery1.htm

[4] Paul B. McBeth, Deon F. Louw, Peter R. Rizun, and Garnett R. Sutherland, *Robotics in Neurosurgery*, The American Journal of Surgery, 188 (Suppl to October 2004) 68S – 75S

[5] Jingke Yu, Rong Liu, Houxiang Zhang and Jiawei Zhang, *Design and Development of an Assisting Robotic Arm in Minimally Invasive Breast Surgery*, Sanya, China, December 15-18, Proceedings of the 2007 IEEE International Conference on Robotics and Biomimetics, 2007

[6] Kanako Harada, Kota Tsubouchi, Masakatsu G. Fujie and Toshio Chiba, *Micro-manipulators for Intrauterine Fetal Surgery in an Open MRI*, Barcelona, Spain, Proceedings of the 2005 IEEE International Conference on Robotics and Automation, April 2005

[7] Yoshio Yamamoto, *Development of Concentric Micro Manipulation System*, Monterey, California, USA, 24-28 July, Proceedings of the 2005 IEEE/ASME International Conference on Advanced Intelligent Mechatronics, 2005

[8] P. Corke, *MATLAB Toolboxes: Robotics and Vision for Students and Teachers*, IEEE Robotics & Automation Magazine, pp. 16-17, December 2007

[9] P. Corke, *A Robotics Toolbox for MATLAB*, IEEE Robotics & Automation Magazine, Vol. 3, pp. 24–32, September 1996

[10] F. Cepolina, *Development of Micro Tools for Surgical Applications*, Ph.D. Thesis, Universita' Degli Studi De Genova/ Uiversite Piere Et marie Currie, Paris 2005

[11] John J. Craig, *Introduction to Robotics Mechanics and Control*, 3rd edition, Pearson Prentice Hall, 2005

[12] R. K. Mittal and I. J. Nagrath, *Robotics and Control*, Tata McGraw Hill, 2005

[13] Richard M. Murray, Zexiang Li, S. Shankar Sastry, *A Mathematical Introduction to Robotic Manipulation*, CRC Press Inc, 1993

[14] Khaled Tawfik, Atef A. Ata and Wael A. Al-Tabey, *Kinematics and Dynamics Analysis of Micro-Robot for Surgical Applications*, World Journal of Modelling and Simulation, Vol. 5 (2009), pp. 22-29

[15] Bruno Siciliano, Oussama Khatib et all, *Handbook of Robotics*, Springer, 2008

[16] Victor M. Becerra, Callum N. J. Cage, William S. Harwin and Paul M. Sharkey, *Hardware Retrofit and Computed Torque Control of a PUMA 560 Robot*, IEEE Control System Megazine, pp. 78-82, October 2004